International Journal of Applied Environmental Sciences
ISSN 0973-6077 Volume 5, Number 2 (2010), pp. 297–316

http://www.ripublication.com/ijaes.htm

Characterizing Mobile Emissions by on-board Measurements

Salvador Enrique Puliafito*[a], Miguel Angel Gantuz[b] and José Luis Puliafito[b]

[a]Conicet / Universidad Tecnológica Nacional , Rodríguez 273, 5500 Mendoza, Argentina
[b]Universidad de Mendoza, A. Villanueva 773, 5500 Mendoza, Argentina
[*]Corresponding author E-mail: epuliafito@frm.utn.edu.ar

Abstract

This paper presents a “bottom-up” characterization of emissions from mobile sources. It focuses on gridded models that rely on data collected by on-board measuring systems. In order to handle the data and to construct the emission model, a new concept is proposed that consists in assigning proper “emissivity” factors to roadways. These factors consider road transport emissions not only as a consequence of vehicles alone, but also, to some extent, of the road segment itself. Within bottom-up models, the on-road measurement is probably the most realistic approach, particularly when compared to the classical dynamometer testing, because the vehicle is measured as it travels in a given roadway. However the principal drawback is the difficulty to handle the data gathered by the measurements and to properly incorporate it to an emission model. As the roads are here characterized as emitters, a robust description of the distribution of emissions at a spatial and temporal level is possible, contributing to obtain more accurate representations of ambient conditions at a micro scale, its temporal variability and compliance to air quality standards. This paper presents a discussion of the experimental results in the city of Mendoza, Argentina, as well as a general methodology to derive gridded emission models for mobile sources using the concepts previously introduced.

Keywords: Atmospheric pollution, mobile sources, gridded emission model, on-board measurement, characterization of roadways.

Introduction

Air quality simulation models are currently organized under a Geographical Information System (GIS) that helps to handle the data and to represent the results in contour maps of pollutant concentrations. This type of model is represented in a gridded form, where the concentration of a pollutant at each cell depends on its own emission sources plus the concentration coming from the atmospheric dispersion of sources located in other cells. Air quality models are organized starting at the emission model, which describes how and where the pollutants are expelled into the atmosphere. Emission models of fixed sources are rather simple, and are directly related to dispersion models. Instead, emission models of mobile sources are intrinsically variable in the compositional, temporal, and spatial dimensions, so that connecting them to dispersion models is a more difficult task. Emission models of mobile sources can adopt the forms of top-down or bottom-up approaches [1].

Top-down approaches are methods derived from regional inventories of air pollution, particularly useful in cases of insufficient information on vehicular use. These begin evaluating the total emitted mass of a certain pollutant, through the consumption of fuels in a given region and period of time (usually given on a yearly basis). From this standing point, the average emission of vehicles, as a function of velocity, can be calculated using information such as number and distribution of inhabitants, average number of trips and driving distances, composition of the automotive park, and fuel consumption factors. The emission can then be organized in a gridded form (gridded emission model) by evaluating the geographical distribution of vehicles and their average velocity ([2, 3]).

Recently, greater interest has been shown in gridded emission models using a bottom-up approach, focusing on the computation of emissions in small areas or at a micro scale. In a bottom-up approach, the emission in a given segment length of roadway is calculated as the number of vehicles per unit of time (vehicular flux) by a proper emission factor given in g/km. A gridded emission model needs for each cell a traffic model and an emission factors model. The first is a model of the average vehicular fluxes, obtained from considering driving distances per vehicle, elapsed time, averaged speed and vehicular density (four step classical models); the emission factors model accounts for the emission due to the various types of vehicles, fuels, velocities and uses like the COPERT IV model [4]. There are several methodologies commonly used to generate and validate emission factors, each with its advantages and drawbacks [5]. Within the top-down approach one might consider the tunnel studies, the inverse modelling, and the chemical mass balance (CMB), while within the bottom-up approach: the dynamometer testing, the remote sensing, and more recently the on-road measurements. Dynamometer testing has been the more widely used source for deriving emission factors for different pollutants. These depend mainly on the type of vehicle, fuel, and speed, and are obtained in laboratory from dynamometric tests performed with standard driving cycles (FTP, I/M 240, ECE R15, EUDC, and others).However, it is well known that emission factors depend on many other factors, such as the driving conditions, the physical characteristics of each street, and more importantly, the traffic imposition. For such reasons, the on-road measurement is probably the most realistic approach, particularly when compared to the classical dynamometer testing, since the vehicle is measured as it travels in a given roadway. The measuring device may be installed inside the vehicle or carried behind. Although these are being recognized as the best way to observe the true behaviour of vehicular emissions [6, 7], it is still an open matter how to manage the data in emission models and take the best advantage of the gathered information. The U.S. Environmental Protection Agency (EPA) is also considering new generation models for mobile sources using on-board transportable equipment [8].

In this paper, a novel bottom-up method is proposed for modelling the emission from mobile sources, using on-road measurements. It is based on the characterization of roadway segments by obtaining proper emission factors according to their own situation. This implies viewing emissions to be caused not only by vehicles, but also, to some extent, by the roadway segment it self. The developed case study was carried out in the city of Mendoza, an urban region of about 850,000 inhabitants located at the foot of the Andes Mountains, 32.8° South latitude and 68.8° West longitude in the Province of Mendoza, western Argentina.

This paper is organized as follow: A first section is devoted to the proposed model and the general methodology of characterization; a second section shows the experimental set-up and some results are presented. The discussion of the underlying theory and justification of results are given in following section. It also includes the generation of gridded emission maps for the case study area. Finally, the last section presents the conclusions.

Methodology and Materials

Roadway characterization

This section presents a different approach to the determination of emission factors, based on the roadway characterization. The total emission in a specific segment of a roadway, for a given contaminant and for a given time, is usually calculated as:

$$E_t = e\,N\,l = \left(\sum_i e_i N_i \right) l \qquad (1)$$

where E_t is the total emission in [g/h], e is an averaged emission factor for all circulating vehicles in [g/km]; N is the vehicle density [veh /h]; and l [km] is the length of the street segment under consideration. The third member of Eq. (1) considers explicitly the contribution of different types of vehicle technologies and fuels (i.e gasoline**;** gasoline with a three way catalyst; natural compressed gas; diesel), with e_i and N_i the average emission factor and vehicle density of group i of the vehicle park, respectively. The accuracy of eq. (1) is limited by the variability and uncertainty in the determination of the emission factors [7] but less attention has been paid to the quantification of the variability and uncertainty of emission factors along roadways [9]. To account for the variability, the different type of factors should be stated explicitly in a generalized emission equation. For example, the emission factor of a given group of the vehicle park can be expressed in terms of a reference value measured with a test vehicle in normalized conditions as:

$$e_0 = f_a\, f_d\, f_v e_b \qquad (2)$$

where f_a , f_d are the ambit and driving variability factors, f_v the vehicle variability factor and e_b the measured emission factor. The total emission in eq. (1) can be referred to the emission of the said group by doing:

$$E_t = e_0 \left(\sum_i C_i m_i \right) N l \tag{3}$$

where C_i and m_i are the relative emission factor and relative vehicle density of group *i*, and e_0 the emission factor of the reference group. Incorporating eq. (2) in eq. (3), the total emission of a given contaminant can be then rewritten in the following way:

$$E_t = f_a f_d \left(f_v e_b \right) \left(\sum_i C_i m_i \right) N l = \bar{e}_b R N l \tag{4}$$

The third member is a synthetic way of expressing the total emission where $R = f_a f_d$. As the parenthesis (f_v e_b $\sum$ C_i m_i) represents an average emission factor $\bar{e}_b$ of the park (obtained in some normalized conditions), then R can be interpreted as the *emissivity* of the roadway segment itself, since the total emission will change according to the particular ambit and driving conditions given by the segment.

The generalized emission equation given in (4) can be used to derive a method for characterizing the emissions of mobile sources of an urban area, by describing the emissivity R of its roadway segments; the size of the roadway segments can be selected based on the characteristics of the district area and the spatial scale of the study. This characterization is based on a single micro scale level, matching in one step traffic and emissions. The emissivity R can be determined experimentally segment to segment as the relation:

$$R = e_r / e_b \tag{5}$$

where e_r is the emission per kilometer measured on-board a test vehicle in the roadway segment, and $\boldsymbol{e_b}$ is the emission per kilometer of such vehicle measured in certain normalized conditions. A simple and suitable way to determine $\boldsymbol{e_b}$ is also by an on-board measurement in a reference or *basal pathway*. The basal pathway is a selected trajectory where a constant velocity and low emissions can be achieved for several kilometres. This ensures that basal emissions can be truly taken as reference since they are gathered under a repeatable test with the same vehicle and on-board equipment. In such way, a practical study of the emissions at a given city or region can be basically accomplished by the following procedure:

(1) Select a representative lot of cars for the area under study, in terms of classes of technology/fuel, engine sizes and age.
(2) Choose a pilot or reference car, which will be loaded with the on-board equipment and will characterize the different streets and highways.
(3) Select a basal pathway and measure the exhaust emissions. All vehicles of the test group must run through this pathway in order to calculate the f_v and C_i factors.
(4) Measure different types of roads and street segments with the reference vehicle.
(5) Refer all measured emissions of the reference vehicle to the basal pathway, calculating the R factor.

(6) Calculate the emission of the segments using Eq. (4).
(7) Associate the roadway segments to geographical cells and build a gridded emission map.

Each of these steps will be discussed in more detail, for the case study, in the following points.

The on-board measurement system

The system was conceived to measure and record exhaust gases, speed and geographical position of the vehicle on the selected trip. It was integrated with the following parts:

(a) A commercial four-gas analyzer LH 5169: Carbon monoxide (CO), Carbon dioxide (CO_2), total hydrocarbon (HC), and Oxygen (O_2). It also detects engine revolutions (rpm), and the air/fuel combustion relation (λ). CO and HC (in equivalent propane or hexane) are detected by non- dispersive infrared absorption measurements, while a long duration electrochemical transducer measures O_2. The range and resolution of the measurements are: CO_2 (0,0 - 18,0 % vol; 0.1%), CO (0,00 - 8,0 %vol; 0.01%), O2 (0,00 - 25,0 %vol; 0.02%), HC (0- 2000 ppm; 1 ppm). An inductive clamp detects the rpm and the factor lambda is calculated with three decimals. It has autozero and automatic and continuous purge of water. There is a complete data gathering and transfer to a PC at more than 1 sample each 3 seconds. It fulfils or surpasses recommendation ISO3930/OIML R99 class II [10], which contemplates oxygen measures, and the EC norms for electromagnetic compatibility and electrical security.
(b) A GPS receptor connected to the laptop computer detects and transfers the velocity and position of the vehicle at a rate of one sample per second, with resolutions better than 0.3 m/s and 100 meter.
(c) A laptop computer with several programs to control the system and to store the incoming data.
(d) A power converter (12V DC / 220 V AC)

Selection of the roadway characterization elements

Pilot roadways: Different types of urban road segments need to be characterized, according to the street hierarchy of the metropolitan area of Mendoza (Figure 1):

(a) Primary roads are main intra county, suburban areas or interregional highways connecting main town poles in the metropolitan area, with a high traffic imposition (15,000-20,000 veh./day), a high average speed of around 48 km/h, and a maximum speed around 80 km/h.
(b) Secondary roads are main streets connecting important urban district areas, with a high vehicle density (8,000 – 12,000 veh./day), with traffic lights regulating most of the intersections, and a low average speed (10-20 km/h).
(c) Tertiary roads are mainly residential streets with a low vehicle density (< 5000 veh/day), very few o no traffic lights regulating the intersections, but in some cases with the presence of speed limiters, presenting a low–medium average speed (20-25 km/h).

The selected roadway segments included the three hierarchies. Tests were performed over all pilot roadways several times at different times of the day with higher and lower traffic conditions and different ambient conditions (weather, temperature, pressure, etc), adding more than 100 tested pathways.

Basal pathway: The basal route must be driven at a constant speed (40 km/h), in a straight road with null slope, at the highest possible gear (transmission ratio) and with the motor in a normal temperature in the hot phase regime. This can be easily accomplished in a low transit road, with only the aid of the odometer of the car. As the speed and emissions are almost continuously recorded, mean values with very low dispersion can be achieved when the test is conveniently repeated several times. In the case study a suitable avenue was selected (J.J. Paso Av.); the fourth gear was adopted in vehicles with gearboxes with five speeds and the third in gearboxes with only four speeds; for tested vehicles that did not behave well in the normalized gear, one lower gear was selected.

Test vehicles: The test group was constituted with gasoline and natural compressed gas vehicles. To represent the active vehicular park of the city as much as possible; ten units were selected, (from a preliminary set of sixteen test vehicles), according to their age, engine size, feeding technologies (carburetor, monopoint injection, and multipoint injection), maintenance condition, and the possibility of testing two types of fuel in some of them, and the use of catalysers in others. Their usage ranged from 75.000 to 180.000 km. The gasoline vehicles were fuelled both with 95 and 97 Octane fuel (Left side Table1).

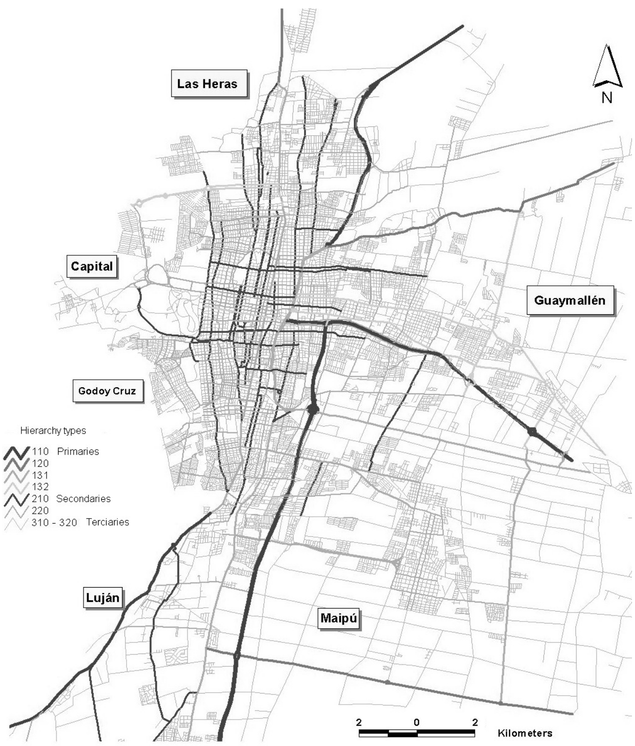

Figure 1: Street hierarchy of Mendoza Metropolitan Area.

Table 1: Summary of the test group of gasoline vehicles and basal test.

Test group					Basal test				
N°	**Description**	**Engine Type**	**Engine Size (l)**	**Feeding technology**	**Veloc. (km/h)**	**RPM**	**Gear**	**eCO (g/km)**	**eHC (g/km)**
1	FORD K	Gasoline Catalyst	1.0	Multipoint injection	40.05	1672	4	0.25	0.11
2	FIAT 147	Gasoline	1.3	Carburetor	41.53	1619	4	45.22	1.61
3	FIAT VIVACE	Gasoline/ NCG	1.3	Carburetor	40.79	1600	4	30.54	1.13
4	FORD FIESTA	Gasoline/C atalyst	1.3	Monopoint injection	41.05	1593	4	7.16	0.86
5	RENAULT 9 (1)	Gasoline/ NCG	1.6	Carburetor	42.60	1370	4	5.24	1.46
6	RENAULT 9 (2)	Gasoline/ NCG	1.6	Carburetor	40.37	1566	4	54.34	2.43
7	FIAT UNO	Gasoline/ NCG	1.6	Carburador	40.90	1658	4	73.25	1.18
8 (REF)	ALFA ROMEO 164	Gasoline	2.0	Multipoint injection	42.23	1364	4	30.46	1.43
9	RENAULT 21 NEVADA	Gasoline/ NCG	2.0	Carburetor	35.81	1407	4	31.83	1.42
10	FORD F150	Gasoline/ NCG	3.6	Carburetor	39.69	1685	3	21.47	2.91

General Basal Test Results	**Emission per cylinder capacity**		**“Mean” vehicle (1.81 liter)**	
	eCO/CIL (g/liter/km)	**eHC/CIL (g/liter/km)**	**eCO (g/km)**	**eHC (g/km)**
Mean values	20.44	0.91	37.01	1.64
Standard deviation	15.06	0.288	27.28	0.52

Experimental Results

Calibration of the on-board measurement system

In order to compare the monitored emissions by the on-board system against other referential measurements, a three step calibrating procedure was performed:

(a) In the first step all test cars were driven on the basal pathway and their emissions were measured with the on-board system. The basal emissions of each test vehicle were then compared with the reference vehicle in order to check internal consistency, and also to intercalibrate the vehicles. The right part of Table 1 shows the results of the basal emissions for the group of vehicles.

(b) In the second step, a 2 liter engine vehicle of the test group (Renault 21) was tested under an “on road” I/M240 test cycle (called here IEMA 240); the driver reproduced the normalized cycle in a low traffic density highway, with the aid of a computer displaying time, velocity, and required gear to perform the cycle; the software was particularly developed for such test. Figure 2 shows the high correlation of the actually performed IEMA 240 with the standard I/M 240. The resulting total CO/HC emissions were compared to those obtained from a 2.3-liter vehicle in a standard I/M240 test cycle (30 tests), performed on a homologated dynamometric facility in Buenos Aires, Argentina (Laboratory for the Control of Vehicular Gaseous Emissions - LCEGV).

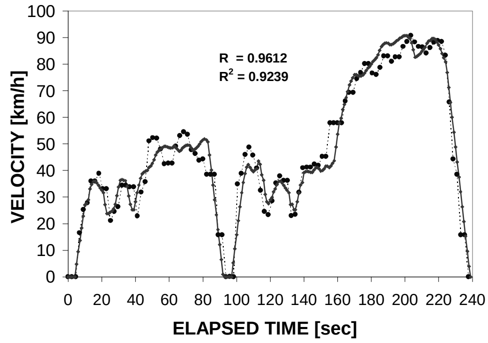

Figure 2: Comparison between the I/M 240 (continuous) and the IEMA240 (dashed) driving cycles. The IEMA240 cycle was performed on- road in a low traffic path in a highway.

(c) Finally, in the third step, a "virtual" I/M 240 test was constructed using data gathered in all roadway tests with the reference vehicle, and also compared to the LCGEV results. To do this, all emission data were first classified as a function of the velocities and gear relations performed in the roadway tests; the average emission factors and dispersions calculated from such table were then applied to the sequence of velocities and gear relations specified in the I/M 240, thus permitting the calculation of the corresponding total emissions.

Table 2 shows the values for the Renault 21 (IEMA 240), Alfa Romeo 164 (virtual I/M240) and the LCEGV vehicle (standard I/M 240), laying all three vehicles in the same range of measurements. This calibration procedure not only validates the on-board system itself, but also verifies the basal intercalibration of vehicles; this means that within the group dispersion, all the roadway segments can be characterized with any of the cars of the test group. This latter allows the comparison of all the real routes with the basal route, particularly by means of the reference vehicle.

Table 2: Comparison of emission results with the LCEGV test.

PARAMETER		VEHICLE		
		LCEGV I/M 240	**Renault 21 IEMA 240**	**Alfa Romeo virtual I/M 240**
CO g/km	Mean	50.92	59.74	68.20
	Mean – std. dev.	43.47	--	33.39
	Mean + std. dev	58.36	--	103.00
HC g/km	Mean	3.61	3.60	2.30
	Mean – std. dev	2.38	--	1.36
	Mean + std. dev	4.84	--	3.24

Characterization of roadway segments: the emissivity factor R

The following test measurements show how the emissivity *R* varies according to the different characteristics of the street segment and its traffic imposition.

Emission variation due to the street slope: In order to study the impact that the slope of a street has on emissions, several measurements were done on a road with a slope of 3.82 %, without traffic. During the way up, emissions increased 2.48 times in terms of CO (148 %) and 1.33 times in terms of HC (33%) with respect to the basal pathway. During the down slope trajectory, CO decreased 40 % and HC increased 143%. The increase in HC and CO during the way up is due to the bigger power demand which increases the fuel consumption. However, downwards, when less power and fuel are needed, only CO emissions are reduced, verifying instead even a bigger increase of HC emissions. This may be explained as an incomplete combustion, or ignition failure, due to a poor mixture [11]; the average air/fuel combustion relation λ compared to the basal pathway decreased 14 % during the way up, and increased 18% during the way down with a 29% decrease in CO2 and 55% increase of O2. This is why the basal pathway has been chosen at no slope.

Variation of R associated to road hierarchy: Dynamical changes to the motor regime are imposed by any obstacles to traffic's fluidity, as traffic lights, intersections, pedestrian crossings, side parking and number of available lanes. On primary roads the emissions increase 1.9 times in CO and 2.01 times in HC with respect to the basal pathway; on secondary roads the emissions increased, on average, 4.7 times for CO, and 7.4 times for HC with respect to the basal pathway; on tertiary roads the emissions of CO and HC are, on average, 2.6 and 4.6 times higher, respectively, with respect to the basal pathway. Speed limiting devices or street irregularities can also strongly affect emissions, by changes on the dynamical regime of the motor. In order to check this, a 2.42 km long roadway segment in a typical residential district was taken (tertiary route) simulating halting at the rate of once per block (around 100 m) reducing the travelling speeds to less than 5 km/h. The emissions were compared to those obtained in the same routes but without stop devices under normal traffic conditions. Under these conditions, CO emissions increased an average of 3.26 times, while the HC emissions increased 1.85 times.

Variation of R due to traffic changes; the temporal factor T_m: Ideally, the emissivity *R* and the traffic flow *N* are considered in Eq. (4) as independent variables. As traffic flow approaches to the congestion limit or capacity of a given street, it imposes changes in the average dynamic regime of vehicles' engines and consequently also over the emissions. Therefore, some parametrical dependence between *R* and *N* can be expected. To investigate this aspect, the emissivity *R* was measured in different streets under considerable changes of traffic flow, which normally occur at different hours due to the urban activity cycles. Thus, this time variation on *R* can be described by means of a temporal modulation factor T_m, which can be defined as the ratio between the emissions of a given vehicle, on the same path, at normal and rush hours. Table 3 displays the results of emissions changes in downtown streets of Mendoza at the noon peak (12:00 –13:30) and at a low transit hour (around 23:00). The resulting T_m is in the order of 0.8 for both polluting agents. This variation of *R* happens almost exclusively in downtown zones and in other specific congested places (surrounding schools, banks, commerce, offices, etc.). In residential tertiary streets, and highways the emissivity does not differ much in different hours, since vehicular congestion is not usually reached. Thus the roadway segments can be mostly described adopting constant *R* values; and when necessary, variations of *R* should be accounted by means of the temporal modulation factor T_m.

Table 3: Variation of emission factors with traffic and the resulting temporal factors in downtown secondary streets ($\boldsymbol{T}_m$= normal hours emission / rush hours emission).

Street Name	eCO g/km		eHC g/km		R_{CO}		R_{HC}		Temporal factor	
	Normal	Rush	Normal	Rush	Normal	Rush	Normal	Rush	$T_{m\,CO}$	$T_{m\,HC}$
COLON	82.94	100.11	5.65	7.16	2.72	3.29	3.94	5.00	0.83	0.79
RIOJA	84.12	104.49	5.82	8.03	2.76	3.43	4.07	5.61	0.81	0.82
SAN MARTÍN	98.06	133.69	7.16	9.43	3.22	4.39	5.00	6.59	0.73	0.76
								Average:	0.79	0.76

The influence of other factors in the characterization of roadway segments

Although the characterization of each type of street was performed mainly by the reference vehicle, most of the roadway segments were also characterized with the other vehicles of the test group in order to check the correspondence in measurements and to calculate the different factors in eq. (4).

The vehicle variability factor f_v**:** This factor f_v (4) can be interpreted, as a normalizing factor that stands for the rate of the average emissions of the test group to the emission of the reference car. This is determined from basal emissions, with all pilot vehicles running on the basal pathway. Ideally f_v should be a constant independent from any other cause of variability, particularly *R* and *N*; however, as the dynamical response of the engines also depend on their technology, age and point of adjustment, some interdependence can be presumed. To investigate this interdependence, the emissions of the test group of vehicles were measured on secondary and tertiary roadways, and compared to the reference vehicle on the same paths under similar conditions. Table 4 shows the average emission values and the variation of the factor f_v. In fact, this factor increases as the transit imposition grows; in other words, the group presents greater dispersion in its emissions as traffic and ambit become more complex. Nevertheless, the increase is rather low for both contamination components, despite the big variation of the emissivity factor *R* in each case. This fact emphasizes the assumption that, on one side the *R* factor can be properly measured with the reference car, and on the other side *R* is mainly a property of the roadway type.

Table 4: Mean values of the emissions for the entire vehicle test group for secondary and tertiary roads. Note that the normalizing factor $\boldsymbol{f_v}$ remains almost unchanged despite the very different ***R*** factor in each case.

	Secondary roadways (downtown) aver. speed 10.14 [km/h]		**Tertiary roadways (residential)** aver. speed 24.29 [km/h]	
Emissions	**CO**	**HC**	**CO**	**HC**
Mean emission factor	156.36	11.89	86.45	7.46
Emission standard deviation	87.61	6.19	57.51	4.03
Emission standard deviation [%]	56%	52%	67%	54%
Factors	**CO**	**HC**	**CO**	**HC**
Emissivity factor ***R***	4.70	7.42	2.60	4.65
Normalizing factor $\boldsymbol{f_v}$	1.17	1.26	1.15	1.14

The use of others fuels and catalysts (factor C_i): In Eq. (4) factor C_i represents the relative emission factor of a given group of fuel/technology. Again, in practice, it can be interpreted as an indicator representing the rate of emissions of a given fuel subgroup to the reference fuel subgroup (in this case gasoline vehicles), measured under basal conditions. In order to check the behaviour of C_i with respect to different pathway types, measurements were performed in secondary and tertiary roads, using the vehicles of the test group with natural compressed gas (NCG) and the gasoline vehicles equipped with 3-way catalyst. Since several of the selected vehicles had a dual fuel system, tests were performed on a group of streets using gasoline and NCG alternatively. The average measurements of the group showed that with NCG the emissions decreased approximately by 90% for CO and 60% for HC, for all pathways. Similarly, when comparing the average emissions of non-catalytic vehicles with vehicles using a 3-way catalyst, reductions of 96% for CO and 90% for HC were obtained, mostly independently of the pathway type. The same rate of reductions for NGC and catalyst were measured independently by national vehicular emission laboratory (LCEGV) in Buenos Aires, under IM/240 test cycle on dynamometer.

As the variation of the C_i factors with respect to the different pathways is weak, average values can be used in practice for both cases, without the need of altering the measured emissivity factors of the streets.

Results and Discussion

The experimental measurements show, that the emissivity R of the streets segments can account for an important part of the variability of the emissions in an urban area. It is important to compare these results to the estimations based on the emission factors gathered by dynamometer testing. These can be represented by the following equation [1]:

$$e(v) = A_p \cdot v^{-B_p} . \qquad (6)$$

For non-catalyst vehicles with carburettor (CORINAIR Pre-ECE) the corresponding CO and HC parameters are A_{CO}= 281, B_{CO}= 0.63 and A_{VOC}= 30.34, B_{VOC}= 0.693, being e [g/km] the emission factor, v the average velocity [km/h] of the test. Fig. 3 shows that the CORINAIR Pre- ECE curves tend to underestimate emissions of HC and CO, mainly because of the *mode hops* given by the experimental results, depending on the considered type of roadway segment. These differences are relevant when considering that emission factors from IEMA 240 test cycle (average speed of 47 km/h; eCO= 59,74 gr/km; eHC=3,60 gr/km) are concordant to the top-down average values accounted for several European countries (average speed of 57 km/h; eCO= 46,5 gr/km; eHC= 4,03 gr/km) [1].

Several authors have discussed the limitations of driving cycles to represent real urban conditions, since they underestimate the emissions in the urban area [12,13]. Some of these authors have also proposed new methodologies to determine better driving cycles based on the statistical analysis of stochastic processes. Indeed, the different speed distribution of each type of road segment provides a detailed insight of the differences seen above. Fig. 4 shows a frequency distribution of the instantaneous speed for each type of pathway. The first sector, with velocities under 5 km/h, can be characterized as a stop-go process, while the second, with speeds above 5 km/h, as a running process. For example, for downtown streets, more than 50% of the time goes by under stop and go conditions, while for residential roads the stop-go conditions only represent 27% of the time. For comparison's sake, the same figure shows the basal pathway (with an almost normal speed distribution) and the I/M240 driving cycle, with a speed distribution that differs quite a lot from the real driving distributions performed in the downtown and in the residential areas. The latter can be more properly associated with highway conditions.

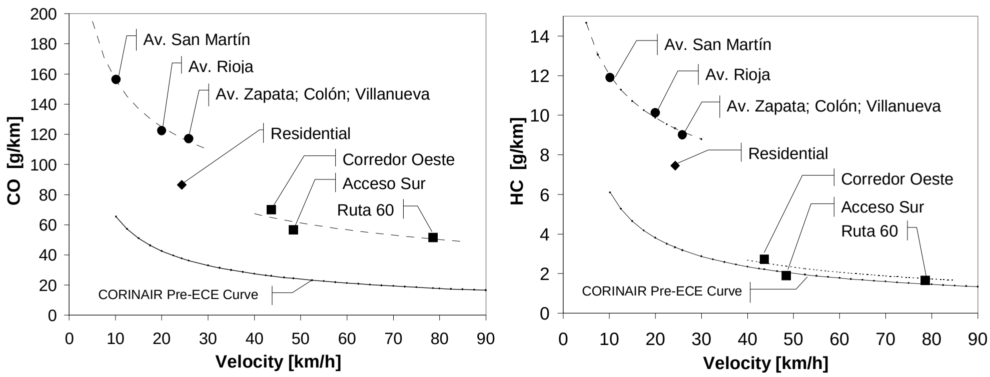

Figure 3: Comparison of average experimental results with CORINAIR Pre-ECE curve, showing a stepwise distribution: a) (Left) CO Emission (gr/km); downtown averages (Av. San Martín, Rioja, Zapata) are distributed on a potential curve $\boldsymbol{e} = 326{,}6\ \boldsymbol{v}^{-0{,}3206}$ ($R^2 = 0{,}9838$) while highways and corridors averages (Corredor Oeste, Acceso Sur, Ruta 60) are distributed on a potential curve $\boldsymbol{e} = 318{,}6\ \boldsymbol{v}^{-0{,}4217}$; residential averages are situated on a mid level. b) (Right) HC Emission (gr/km); the distribution is very similar to CO, downtown averages are distributed on a potential curve $\boldsymbol{e} = 23{,}195{,}6\ \boldsymbol{v}^{-0{,}2854}$ (R^2= 0,9732) while highways and corridors averages on a potential curve $\boldsymbol{e} = 30{,}548\ \boldsymbol{v}^{-0{,}6752}$; residential averages are also situated on a mid level.

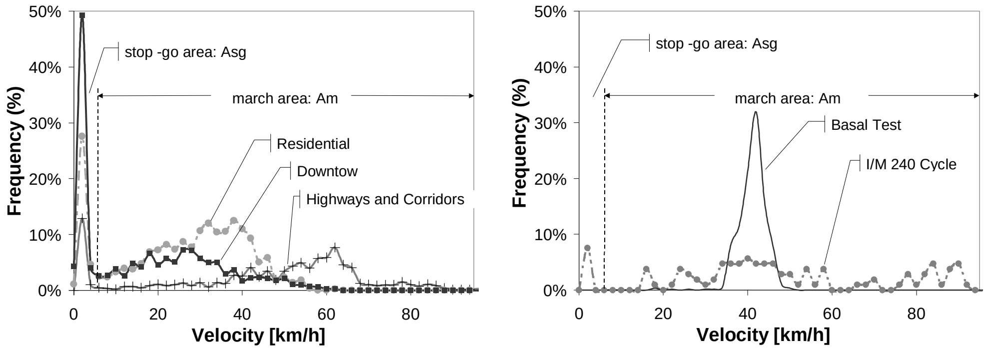

Figure 4: Frequency distribution of vehicular speed traveling in different pathways types: a) (Left) Urban pathways by hierarchies. b) (Right): I/M 240 cycle and basal pathway test.

The emissivity of pathways and the frequency distribution of velocities

The dependence of the emission with the average velocity and its frequency distribution is well captured by the emissivity factors. This starts at the instantaneous emission ε [g/s], which is proportional to the fuel consumption and hence to the power developed by the motor:

$$\varepsilon = \alpha \cdot P = k \cdot \omega \tag{7}$$

where α [g/W.s] is a proportionality constant (depending on the contaminant, the fuel density and the specific fuel consumption) and *P* [W] the power developed by the engine. It can also be expressed as in the third member, where *k* [g] and ω [1/s] are the emission per rotation cycle and the angular velocity of the motor, respectively. Rigorously, *k* must not be taken as a constant but rather as varying parametrically with engine revolutions ω. Expressing the average emission factor as a function of its probability density $p(\varepsilon)$, leads to

$$\int_{\varepsilon_{min}}^{\infty} \varepsilon\, p(\varepsilon) d\varepsilon = \bar{\varepsilon} \cdot \int_{\varepsilon_{min}}^{\infty} p(\varepsilon) d\varepsilon$$

where ε_{min} is the ralenti emission corresponding to ω_{min} and $v \leq v_c$ (stop condition). Considering now that $p(\varepsilon)d\varepsilon = p(\omega)d\omega = p(v)dv$ (again for $\omega > \omega_{min}$, $v > v_c$ and $\varepsilon > \varepsilon_{min}$), the average emission $\bar{\varepsilon}$ of the running process is:

$$\bar{\varepsilon} \cdot \int_{v_c}^{\infty} p(v)dv = \int_{\omega_{min}}^{\infty} k\, \omega\, p(\omega)\, d\omega \approx \bar{k}\, \bar{\omega} \;\rightarrow\; \bar{\varepsilon} \approx \left(\frac{\bar{k}}{\overline{g \cdot \eta \cdot r}} \right) \cdot \frac{1}{\int_{v_c}^{\infty} p(v)dv} \cdot \bar{v} \tag{8}$$

Last equation in (8) shows that the average emission of a pathway depends on the mean velocity $\bar{v}$, as well as on the probability distribution of the velocity $p(v)$. However, it also depends on the response of the vehicle-driver system to the mean driving mode (the factor given by the parenthesis), with *g* being the total gearing relation, η the transmission efficiency, and *r* the dynamic radius of the wheels of the vehicle. The probability distribution of the velocity can be analysed by computing the normalized areas under the stop-go mode and the marching mode for the same driving path; thus:

$$\int_0^\infty p(v)dv = 1 = \int_0^{vc} p(v)dv + \int_{vc}^\infty p(v)dv = A_{sg} + A_m$$

Where A_{sg} is the area under the stop-go mode, and A_m is the area of the running mode. As the average emission factor [g/km] of a given pathway is $e_r = \overline{\varepsilon} / \overline{v}$ the following expression can be written:

$$e_{r(gr/km)} = \overline{\varepsilon}/\overline{v} = \left(\frac{\overline{k_r}}{\overline{\overline{g_r \cdot \eta_r \cdot r}}} \right) \cdot \left(1 + \frac{A_{sg}}{A_m} \right) \tag{9}$$

The emissivity R of the pathway can be obtained dividing (9) by the basal emission $\boldsymbol{e_b}$ in [g/km]:

$$R = \frac{e_{r(g/km)}}{e_{b(g/km)}} = \frac{\overline{(\eta_b\, g_b)}}{\overline{\overline{(\eta_r\, g_r)}}} \cdot \frac{\overline{k_r}}{\overline{k_b}} \cdot \left(1 + \frac{A_{sg}}{A_m} \right) = \frac{1}{\gamma} \cdot \frac{\overline{k_r}}{\overline{k_b}} \cdot \left(1 + \frac{A_{sg}}{A_m} \right)$$

where $\gamma = \overline{g_r} / \overline{g_b}$ stands for the average relative gearing relation of the pathway. If the gearing is always selected optimally for the requested power γ can be taken as a particular constant of the pathway.

Derived from Eq. (7) $\overline{k}_r / \overline{k}_b = (\overline{P_r} / \overline{\omega_r}).(\overline{\omega_b} / \overline{P_b})$, so that the emissivity R can be rewritten as:

$$R = \frac{e_{r(g/km)}}{e_{b(g/km)}} = \frac{\xi}{\gamma \cdot \beta} \cdot \left(1 + \frac{A_{sg}}{A_m} \right) \tag{10}$$

where $\beta = \overline{\omega_r} / \overline{\omega_b}$ and $\xi = \overline{P_r} / \overline{P_b}$ are the relative engine revolution and relative power load of the pathway respectively, since ω_b and $P_b(\omega_b)$ are approximately constant. The product $S_E = \xi / (\gamma . \beta)$ is a non-dimensional specific emission factor, which is responsible for the step-wise distribution of the measured values; it has different amplitudes according to the average gearing relation γ and the relative average revolution β of the pathway type.

It is worthy to notice that Eq. (10) follows the emissivity definition in (4), since ξ / γ depends on the driver response whilst $(1/\beta).(1 + A_{sg}/A_m)$ on the ambit imposition. If instead of using the relative engine revolution β, the pathway average relative speed $\overline{v}_r / \overline{v_b}$ is used, the resulting emission factor

$$E = \frac{\overline{v}_b}{\overline{v}_r} \cdot \left(1 + \frac{A_{sg}}{A_m} \right) \tag{11}$$

Which can be considered as the intrinsic emissivity of a pathway, for it does not depend on the vehicle. As it is shown in Fig. 5.a, the emissivity R_{HC} can be approximated fairly well using σE, with a constant $\sigma = 1.4$. However, in a more detailed view, the data groups are found mostly arranged by segments almost crossing the σE curve due to the S_E modal effect. Fig. 5b show a qualitative simulation of (10) using a potential approximation for R_{HC} and a bell shaped curve for the efficiency of the engine as a function of its angular frequency.

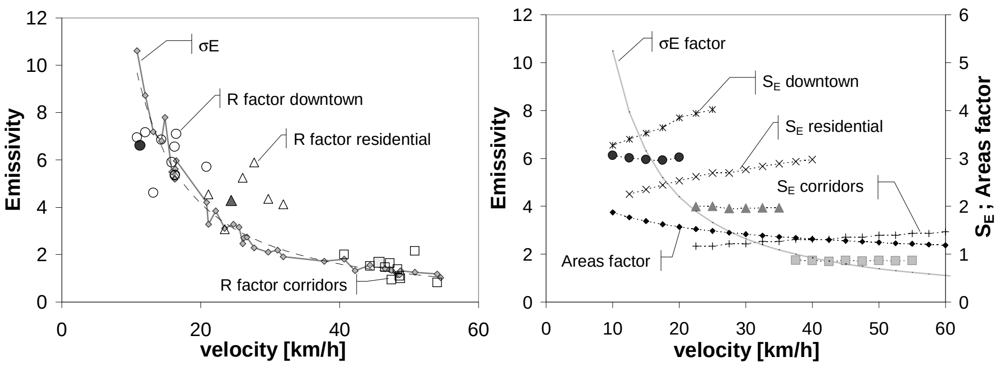

Figure 5: Correlation between the emissivity factor $\boldsymbol{R}_{HC}$ measured in each street and the intrinsic emissivity factor $\boldsymbol{E}$. a) (Left) Experimental results: The HC emissivity $\boldsymbol{R}_{HC}$ for relevant paths measured with the reference car are marked either with circles (downtown streets), triangles (residential streets) or squares (highways and corridors), the same symbols but filled represent the mean values obtained for the entire group of test cars. The potential approximation for all path data is given by $\boldsymbol{R}_{\mathbf{HC}} \approx 188.7\, \boldsymbol{v}^{-1.2535}$ with a correlation factor of 84 % (R^2=0.7026) (dashed line). The continuous line is the E factor unless a constant (σ=1.4), computed by eq. (9) from data of each roadway segment. b) (Right) Qualitative simulation: Explanation for the data distribution of the left figure, using Eq. (8), compared with the potential approximation of σE. The continuous segments (circles, triangles, or squares) represent the resulting R factor for different hierarchies, according to the areas probability factor and the mode hops given by the S_E coefficient (discontinuous segments).

Intrinsic emissivity E and roadway characterization plane

The intrinsic emissivity *E* is not only a good approximation for the real emissivity *R* of the pathways but also a good descriptor of the particular organization of the city and the response of the traffic to it. In fact, the different emission patterns generated at different street types and their associated driving modes can be characterized out of equation (8), splitting it into two inverse variables $\eta = 1/(1+A_{sg}/A_m)$ and $\mu = (\overline{v}_r / \overline{v}_b)$. These two factors can be depicted together forming the *roadway characterization plane*, as shown in Fig. 6, where the pairs of numbers (η, μ) represent each of the measured pathways. This plane immediately gives a categorization according to the above-mentioned hierarchy of streets, since the computed values are organized in well-defined clusters. Moreover, the clusters can be characterized by their relative position; in order to do that, the plane is divided into two sub planes by the line given by the points (0,0) and (1,1): the upper area corresponds to emission values that are dominated by traffic flow imposition, such as in dense traffic highways; while the lower area corresponds to emission values in streets controlled by ambit imposition (intersections, speed limiters, traffic lights, and safe and careful driving) such as in a residential or downtown area.

This plane is not only useful to compare the emission patterns within a given city, but also to compare the relative emission of urban streets, on a city-to-city base. In this sense, this plane could be a useful tool for policy makers and urban planners to analyse, for instance, the results of concrete measures such as traffic rearrangement to reduce vehicular pollution in a given area.

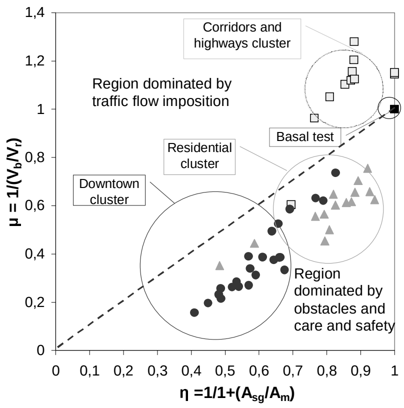

Figure 6: Roadway characterization plane. This has been done splitting the intrinsic emissivity ***E*** in two inverse factors; the figure shows the resulting values of all tests performed in Great Mendoza.

Construction and validation of gridded emission maps

A gridded emission map can be generated, using a geographical information system (GIS), by first dividing the urban area in a rectangular grid; for the case study a georeferenced grid system was used with cells (pixels) of 350×350 m^2. Next step is to divide its streets and roads into representative segments assigning each segment to the correspondent cell. For the case study, approximately 25.000 segments were generated and then characterized with their emissivity *R* and traffic flow *N*. The detailed spatial distribution of traffic *N* is normally unknown, but it can be assigned to the street segments assuming that the city produces a central area of attraction, so that the instant distribution of vehicles exhibits certain proportionality to the distribution of population. Thus the vehicular traffic counting will grow as a function of the distance from the main central area and the street hierarchy, and the velocity *v* inversely proportional, reaching a minimum at congestion points at downtown. Traffic flow and average speed can be expressed by the following logistic type functions, and then adjusted to the measured values at the main intersections [2]:

$$v(i,j) = v_0(j)\exp((d-1))/a)$$
$$N(i,j) = N_0(j)\exp((1-d)/b) \tag{9}$$

where *v(i,j)* (km/h) is the speed at segment *i* and hierarchy *j*; *N(i,j)* is the number of vehicles per day at segment *i* and street hierarchy *j*, *d* is a normalized distance to the central district area (*d*=1 at the central area, *d*=0 at city outer limits); *a* and *b* are scale coefficients that are chosen to match the known data and source destiny surveys, an calibrated with the on board measurements. Table 5 shows the emission factors for HC and CO for gasoline vehicles, applying Eq. (9), for each street segment type. Once the emissions per roadway segments are known, the emissions per cell can be computed as the sum of the segment contributions to the cell, which leads to the gridded emissions maps for HC and CO shown in Fig. 7 and Fig. 8 respectively. It can be seen, as expected, that there are higher emissions at the central district area and along the main access roads. From this emission patterns, it is possible to derive the ambient concentrations using proper dispersion algorithms.

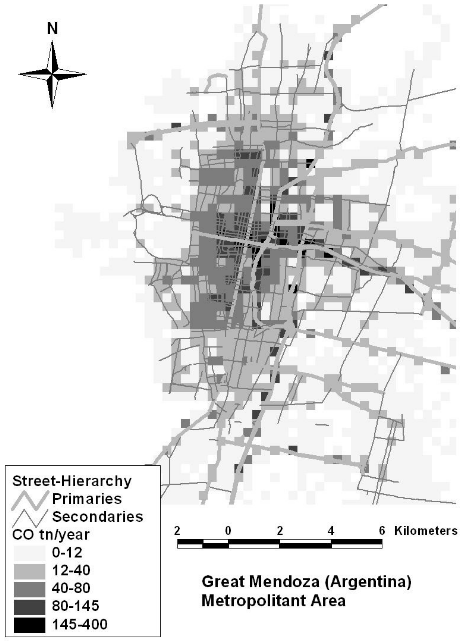

Figure 7: Gridded emission maps for carbon monoxide in tn/year calculated for Great Mendoza, Argentina. The size of the cell is 350x350 m^2.

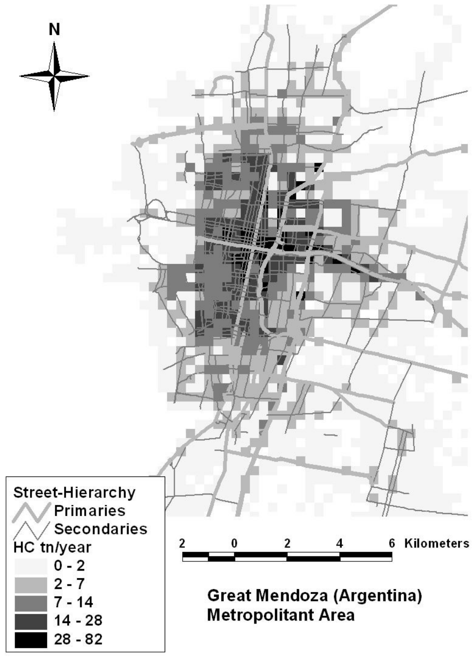

Figure 8: Gridded emission maps for HC in tn/year respectively, for Great Mendoza, Argentina. The size of the cell is 350x350 m^2.

Table 5: Parameters for the vehicular flux and speed, and the average emissions factors for CO and HC (gasoline vehicles), for each type of segment.

Variable	Hierarchy					
	Primary			Secondary		Tertiary
j	110	120	130	210	220	310
v_0	60	40	40	30	25	20
a	1,5	1,4	1,4	1,5	1,5	1,6
N_0	23000	17000	10000	7000	6000	2000
b	0,35	0,3	0,25	0,25	0,2	0,2
e_{CO} (GV) [g/km]	47,9	55	54,1	76,4	81,4	45,1
e_{HC} (GV) [g/km]	3,5	4	2,1	8,3	8,6	7,6

Table 6: Total city emissions calculated for gasoline vehicles (Tn/year): Comparison of methods and sensibility of the total emissions calculated by the bottom-up approach.

	Comparison of methods			**Sensibility of the Bottom-Up approach**		
Pollutant emission	Top-down	Bottom-up	Relative Dif %	Average	Deviation	% Variation
CO [Tn/year]	30,908	33,319	7.8%	31,817	447	1.40%
HC [Tn/year]	5,099	4,293	-15.8%	3,987	48	1.20%

It is also possible to compute the total annual emissions of CO and HC summing up emissions cell-to-cell in a bottom-up approach. The impact of the proper variability of the street segment regime and the uncertainty of its characterization data has been evaluated for the bottom up method using a Monte Carlo analysis (Table 6). It was computed considering random deviations from the corresponding mean value of up to 40% in velocity, 70% in traffic flow and 50% in CO and HC emission factors. This result can be compared with the correspondent evaluations using a top-down inventory, which are estimated from energy consumption and standard emission factors. Table 6 shows the total emissions computed for the gasoline sector for both approaches. The results from the simulation test, demonstrate that the annual mean values are relatively insensitive to random changes at small scale (left part of Table 6).

Conclusions

A “bottom-up” methodology for the determination and estimation of the spatial and temporal distribution of emissions from mobile sources has been presented; it is focused in constructing dynamic grid models for vehicular emissions based on data gathered by on- board measuring systems. A new concept of characterization of emissions has been introduced in order to handle the on-board measurement data, according to which proper “emissivity” factors are assigned to roadway segments. Measurements show that the street segment emissivity factors can be considered rather independently of the actual vehicular flux, even in highly congested segments. Instead, they strongly depend on road hierarchy, so that the emissions can be treated as a consequence not only of traffic density but also of the road segment itself. It has been shown that the intrinsic emissivity factor of a road is an important characterization parameter, for it comprises not only the mean velocity but also the distribution of velocities. This leads to a road characterization plane, where the roadway segments can be described as forming part of clusters, thus defining the emission pattern of a city. The characterization plane may also be used to compare the relative emission of urban streets inter and intra cities. In this sense, this plane could be a useful tool for policy makers and urban planners. The advantage of this type of model is not only that it can provide a robust description of emissions at the spatial and temporal levels, but also that it can help to obtain a better representation of the ambient conditions and their compliance with air quality standards.

Acknowledgement

The author acknowledges the authorities of the Argentine Research Council (CONICET) and the Argentine Technological University (Universidad Tecnológica Nacional) for supporting his research activities. This project was funded by grant PICT 2005 23-32686 from Agencia FONCyT Argentina.

Appendix: List Of Most Used Symbols

Symbol	Units	Description
ϵ_t	[g/h]	Total emission rate of a roadway segment
e	[g/km]	Emission factor (linear)
ε	[g/s]	Emission factor (temporal)
N	veh/h	Vehicle density
l	[km]	Length of street segment
f_a	-	Ambit variability factor
f_d	-	Driving variability factor
f_v	-	Vehicle variability factor
C_i	-	Relative emission factor of a group i of vehicles respect to a reference group
m_i	-	Relative vehicle density of a group i of vehicles respect to a reference group
R	-	Emissivity of a street segment
T_m		Temporal modulation factor of the emissivity
v	[km/h]	Average velocity
γ	-	Basal to pathway average relative gearing relation
ξ	-	Pathway to basal average relative power load
β	-	Basal to pathway average relative engine revolutions
$S_E = \gamma . \xi . \beta$	-	Specific emission factor
A	-	Normalized area under the velocity probability distribution. Sub-indexes: t (total); sg (stop and go): m(march)
E	-	Intrinsic emissivity

References

[1] Eggleston, H.S.; Gaudioso, D.; Gorissen, N.; Joumard, R.; Rijkeboer, R.C.; Samaras, Z.; Zierock, K.H., 1991, "CORINAIR Working Group on Emission Factors for Calculating 1990 Emissions from Road Traffic. Volume 1: Methodology and Emission Factors"; Contract Number B4-3045 (91) 10PH;

Commission of the European Communities, DG XI–EEA Task Force: Brussels, Belgium, 1991.

[2] Gualtieri, G. and Tartaglia, M., 1998, “Predicting Urban Traffic Air Pollution: A GIS Framework”, Transportation Research Part D, Vol. 3, Nº. 5: 329-336.

[3] Puliafito, E.; M. Guevara; C. Puliafito, 2003, “Characterization of urban air quality using GIS as management system”. Environmental Pollution Vol 122, pp 105-117.

[4] Ntziachristos, L., Samaras, Z., 2000, “COPERT III Computer programme to calculate emissions from road transport Methodology and emission factors”, Technical Report No 49, EEA, Copenhagen.

[5] Fujita, E.M., Croes, B.E., Bennett, C.L., Lawson, D.R., Lurmann, F.W., Main, H.H., 1992. “Comparison of Emission Inventory and Ambient Concentration Ratios of CO, NMOG, and Nox in California's South Coast Air Basin”. Journal of the Air & Waste Management Association 42, 264-276.

[6] Frey, H.C., A. Unal, and J. Chen, 2002, “Recommended Strategy for On-Board Emission Data Analysis and Collection for the New Generation Model”, North Carolina State University for Office of Transportation and Air Quality, U.S, EPA, Raleigh, NC.

[7] Frey, H.C., D.A. Eichenberger, 1997, “Remote Sensing of Mobile Source Air Pollutant Emissions: Variability and Uncertainty in On-Road Emissions Estimates of Carbon Monoxide and Hydrocarbons for School and Transit Buses”. North Carolina State University for North Carolina Department of Transportation, Raleigh, NC.

[8] EPA, 2001. “New Generation Mobile Source Emissions Model: Initial Proposal and Issues”, EPA Mobile Source Emissions Modeling Workgroup, Office of Air and Radiation, Office of Research and Development, Region 4, EPA 420-R-01-007.

[9] Wenzel T., Singer B. & Slott R., 2000. “Some Issues in the Statistical Analysis of Vehicle Emissions”; Journal of Transportation and Statistics; Bureau of Transportation Statistics US Dep. of Transportation.

[10] OIML, 2000, “International Organization of Legal Metrology”, www.oiml.org/publications; see also www.iso.org-

[11] Wark, Warner, 1981, “Air Pollution: Its Origin and Control”. 2nd Ed. New York, NY.: Harper & Row Publishers.

[12] Ahn, K., Rakha H., Trani, A.,Van Aerde M. , 2002, “Estimating Vehicle Fuel Consumption and Emissions based on Instantaneous Speed and Acceleration Levels”. J. Transp. Eng., Volume 128, Issue 2, pp. 182-190.

[13] Lin J., Niemeier D. A., 2003- Estimating Regional Air Quality Vehicle Emission Inventories: Constructing Robust Driving Cycles- Transportation Science, Volume: 37 Issue: 3 Page(s): 330 -346.